COMPLETE ANALYSIS AND SIMULATION OF RECIPROCATING PUMPS INCLUDING SYSTEM PIPING

by

Pawan J. Singh

Manager, Advanced Technologies

and

Nateri K. Madavan

Researcher

Pump Group Research & Development

Ingersoll-Rand Company

Phillipsburg, New Jersey

Pawan J. Singh is Manager of Advanced Technologies in the Pump Group Research and Development Department at Ingersoll-Rand Company. He is responsible for conducting research in various aspects of centrifugal and reciprocating pump technology, developing new products and applying advanced analytical techniques to improve existing products. He also serves as a technical consultant to several other divisions of the company manufacturing reciprocating and rotary compressors, expander turbines, and water-jet cutting machinery.

During his fourteen years of tenure in various industries, he has held several senior engineering positions and has made leading contributions to hydroacoustics, ship hydrodynamics, and turbomachinery technologies. He has also served as an adjunct faculty member at the University of Rochester and Widener University, Chester, Pennsylvania.

Dr. Singh received his M.S. (1970) and Ph.D. (1973) degrees in Mechanical Engineering and Aerospace Sciences for the University of Rochester. He has won several academic awards, has published extensively, and lectured internationally. He is a member of ASME and New York Academy of Science.

Nateri Madavan is a Researcher in the Pump Group Research and Development Department at Ingersoll-Rand's Phillipsburg facility. He is active in hydraulic research on centrifugal and reciprocating pumps. His responsibilities include developing advanced computer-based techniques for pump design and analysis, simulation of pump piping systems and research on cavitation damage.

He received the B. Tech degree (1979) from the Indian Institute of Technology at Kharagpur, India, an M.S. degree in Mechanical Engineering (1981) from Iowa State and a Ph.D. degree in Mechanical Engineering from Penn State (1984). Dr. Madavan is the author of several technical publications. He is a member of AIAA and an associate member of ASME.

ABSTRACT

A computer model is presented for the analysis and simulation of a complete reciprocating pump installation. The model takes into account cylinder thermodynamics, valve dynamics, and acoustic pulsations in the suction and discharge piping. The simulation is done in an integrated manner to account for all the dynamic interactions between the various system components. The model can predict cylinder pressure traces, valve motion, pump capacity and NPSHR, system resonance frequencies and pressure pulsations at any specified point in the suction or discharge piping.

Applications of the computer model include use in the rapid evaluation of new pump component designs, understanding pump behavior, designing new pump installations, troubleshooting pulsation problems at current installations and evaluating recommended system modifications.

The focus herein is primarily on the applications of the computer model. A brief outline of the underlying theoretical analysis is also presented. Several comparisons between model predictions and experimental data are presented and shown to be in good agreement. Finally, various aspects of pump operation are discussed in the light of experience gained by applying the computer model to various field problems.

INTRODUCTION

Reciprocating machines date back to the days of the industrial revolution. On the one hand, in certain applications, notably internal combustion engines, constant research and development has kept them at the forefront of technology. Advances in other fields, such as materials, computerized design techniques and microprocessor-based controls are also being constantly incorporated into new designs. On the other hand, in the case of applications such as reciprocating pumps, technological developments have been very slow. In particular, these applications have not fully reaped the benefits of the explosive growth in computers. Work undertaken to improve this latter situation is discussed.

Reciprocating pumps are essentially constant-torque, fixed displacement/revolution machines. Since the flow is independent of the head or pressure rise, these machines are ideally suited for low specific speed range applications, i.e., low to moderate flow capacity and very high head rise. They are used to pump a wide range of fluids ranging from low-

viscosity boiler feedwater to highly viscous crude oils and from high-pressure CO_2 to highly corrosive slurries.

Reciprocating pumps typically run at low speeds and moderate to high discharge pressures. However, present-day industry needs and economic factors are pushing pump speeds and operating pressures to higher levels (in excess of 10,000 psi) than ever before. These requirements are beginning to strain the limits of standard design formulae and empirical correlations that have been carefully honed through years of experience. When such design techniques fail to work, manufacturers resort to a patchwork of analytical and/or experimental techniques, focusing strictly on solving the particular problem at hand.

Two common reliability problems associated with pump operation are valve failures and piping pulsations and vibrations. Valve failures generally result from cavitation or improper valve dynamics. Sometimes, pump operating conditions vary over a wide range, and the valves that perform well at one condition may be totally ill suited at others. Cavitation depends both on valve dynamics as well as piping pulsations. It is, therefore, essential that a good computer model be capable of integrating all aspects of pump operation.

Pressure pulsations in reciprocating pumps and compressors arise from the basic intermittent nature of flow entering and leaving these machines. The flow intermittency may be reduced, but not eliminated, by the use of multiple plunger pumps, with each plunger phased differently relative to the others. While the flow characteristics primarily depend on the pump behavior, the pressure pulsations in the piping depend mainly on the piping arrangement and dimensions. One particularly worrisome aspect of this piping response is the excitation of piping resonances that may amplify otherwise small pulsations by a factor of 100 or more. The pulsations in pump piping systems are generally much higher than those in compressor systems because of the higher density and lower compliance of liquids.

In order to attenuate these pulsations, a wide variety of pulsation dampeners [1] that attempt to isolate the piping system from the pump excitations are in use. The sizing and selection of these dampeners for a particular application is, for the most part, an empirical process based on the experience of the vendor or the user. Analog methods, particularly the Southern Gas Association (SGA) Analog [2], have been used for over two decades to design proper dampeners for
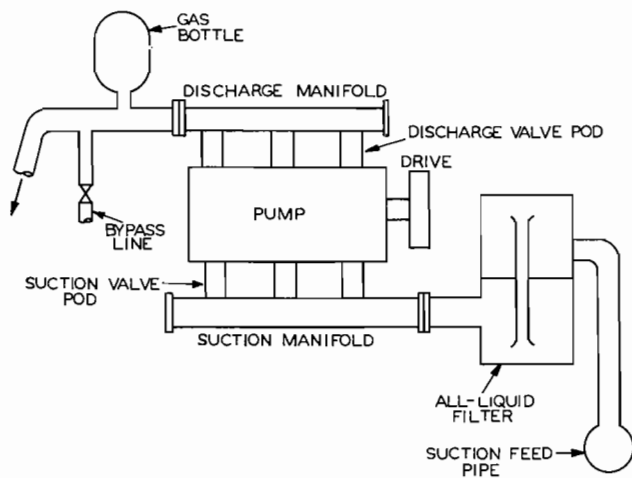
reciprocating compressors and to solve field problems [3]. While these methods have also been used for pumps, new digital techniques are being actively and successfully applied [4] to simulate piping systems. As pointed out earlier, it is necessary to couple the piping response with the pump operation in order to obtain realistic results.

Several years ago, one company decided to adopt a comprehensive approach toward pump technology development. One component of this effort is the development of a new computer program that provides a complete simulation of a reciprocating pump installation. This simulation takes into account the effects of unrestricted suction and discharge piping, pulsation dampeners, valve dynamics, and internal thermodynamics of multiple-plunger, single or double-acting pumps in a unified manner. The model presented follows the pattern of a similar model created for reciprocating compressors and described by Singh [5].

PUMP-PIPING SYSTEM SIMULATION

Theory

A brief description of the theoretical basis for the system simulation along with the underlying assumptions is presented in this section. Additional mathematical details are provided in Appendix 1.

A schematic representation of a triplex reciprocating pump with sample suction and discharge piping is shown in Figure 1. A cross-section of one of the cylinders showing the plunger, which is normally driven by a crank mechanism, is depicted in Figure 2. The automatic suction and discharge valves shown in Figure 2 allow fluid to flow into and out of the cylinder depending on the pressure in the latter.

Fluid Properties

The fluid is assumed to be a single-phase, constant-density, homogenous liquid. Both single- and multi-

Figure 1. Schematic of a Reciprocating Pump, Showing Suction and Discharge Piping Arrangement and Pulsation Dampeners.
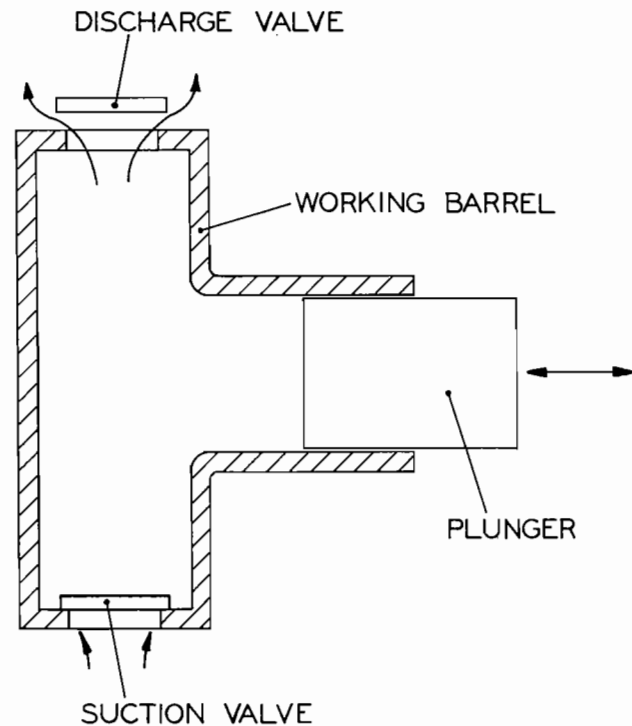

Figure 2. Cross-sectional View of Reciprocating Pump Cylinder Showing Plunger, Suction and Discharge Valves.

component liquids may be specified. During cavitation inside the working barrel, two distinct regions of fluid and fluid vapor are assumed. Fluid properties, viz., density, bulk modulus, viscosity, speed of sound, and vapor pressure are inputs to the analysis.

Cylinder Kinematics

Among the various mechanisms available to drive the plunger, the crank mechanism is the most common. The program thus uses the volume-time relationship (Equation A-1) for such mechanisms as a standard, but a provision for other types of drive mechanisms is also included.

The rate of change of cylinder volume (Appendix A) may be expressed as,.

$$\frac{dV}{dt} = -Apr\left[\mathrm{Sin}\theta - \frac{r}{2l}\,\mathrm{Sin}2\theta\right] \tag{1}$$

Various symbols are described in the NOMENCLATURE. It can be seen that the presence of the connecting rod introduces second order harmonics in the plunger motion. As will be shown later, this has significant and surprising effects on the piping pulsations.

Cylinder Pressure

The rate of change of pressure cylinder pressure is calculated as the net flow into the cylinder control volume multiplied by the fluid bulk modulus (Equation A-4). The bulk modulus is assumed to be constant, corresponding to the mean pressure and temperature, but the program can easily be adapted to account for the variation of bulk modulus and density with pressure and temperature. It might be noted that such variations only become significant at very high discharge pressures (in excess of 10,000 psi for water). When the pressure is calculated to be lower than the vapor pressure, it is set to the vapor pressure value and the cylinder is said to be cavitating.

Valve Dynamics

Both suction and discharge valves are assumed as two separate, single degree of freedom, damped, mass-spring systems (Equation A-5). The pressure difference across the valve lift element acts as the forcing function. While many different types of valves are currently in use, the poppet valve and ball valve shown in Figure 3 are the most common. The pressure distribution around the poppet or ball is calculated by setting up a control volume around the valve lift element and then calculating the pressure at different points along the element. This pressure is then integrated

over the surface to calculate the time-varying net force. Note that forces caused by fluid inertia are generally important in pumps, particularly at high speeds, and should not be ignored.

For multiple-element valves and valves with complex geometries where it is difficult to compute the pressure distribution from first principles, an experimental approach similar to that used for compressor valves [5] may be used. This is a quasi-steady analysis where the net pressure force and flow through the valves are computed from experimentally derived dimensionless coefficients (Equation A-6).

Piping Dynamics

The propagation of acoustic pulsations in the system piping can be predicted by numerically solving the linear, one dimensional wave equation [6] with appropriate boundary conditions. The boundary conditions include junctions where a certain amount of wave energy is reflected back. The combination of transmitted and reflected waves results in standing waves. The wave or pressure amplitude is a function of the acoustic impedance characteristics of the piping system, which in turn is a function of the piping length and diameter, the speed of sound in the pumped fluid, the location of junctions and the type of end conditions. It may help to clarify here that by the term acoustic waves, we are referring to low-amplitude pressure waves that propagate through compression and rarefaction of the fluid medium in a mechanism similar to sound wave propagation. This does not necessarily imply that the useful frequencies are limited to the audible range of sound.

Several techniques for solving the wave equation to predict piping pulsations have been reported in the literature. These include electrical analog [7], lumped parameter [8], finite-difference [9, 10, 11], finite-element [12, 13], method of characteristics [14], and transfer matrix techniques. Among these, the transfer matrix technique is particularly well suited for the digital computer. This technique has received wide attention both in electrical circuit theory [15] and acoustic applications [5, 16, 17, 18, 19] and is the approach adopted here.

In this technique, the piping response is calculated by determining the piping impedance at different exciting frequencies relative to the flow sources and the point of interest. For instance, for a straight piping section the pressure and flow oscillations $\bar{P}_1$ and $\bar{Q}_1$ on the left end of the piping can be related to the right end oscillations $\bar{P}_2$ and $\bar{Q}_2$ in the frequency domain as follows:

$$\begin{bmatrix} \bar{P}_1 \\ \bar{P}_2 \end{bmatrix} = \begin{bmatrix} Z_{11} & Z_{12} \\ Z_{21} & Z_{22} \end{bmatrix} \begin{bmatrix} \bar{Q}_1 \\ \bar{Q}_2 \end{bmatrix} \tag{2}$$

$$\text{or } \bar{P}_i = \sum_j Z_{ij}\,\bar{Q}_j$$

$\bar{P}_i$ and $\bar{Q}_i$ are complex pressure and flow variation vectors and Z_{ij} is the transfer impedance matrix for the piping. Further mathematical details are supplied in Appendix A.

The concept of impedance comes directly from the electrical analogs of flow (current) and pressure (voltage). From Equation (2), the pressures $\bar{P}_1$ and $\bar{P}_2$ can be determined for known flow conditions $\bar{Q}_1$ and $\bar{Q}_2$, provided the impedance matrix Z can be calculated. The matrix Z for a large piping system can be calculated from the piping dimensions and the fluid properties through judicious multiplication of the transfer (or four-pole) matrices for each element. In a sense, the four-pole matrix can be looked upon as a building block that can be combined with other blocks and moved around to
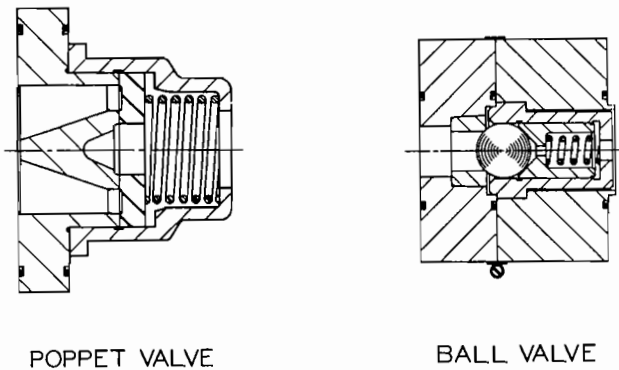

POPPET VALVE   BALL VALVE

Figure 3. Sectional View of a Typical Poppet Valve and Ball Valve.

form the complete piping system. Fortunately, four-pole matrices for common piping elements such as pipes, orifices, choke-tubes, junctions, gas bottles, and all-fluid filters are either available or can be readily calculated to various levels of sophistication. The response of many of these elements have also been compared against test data [16]. This building-block approach makes the transfer-matrix method a very powerful practical tool for calculating piping system pulsations induced by reciprocating machines. The technique can also be used to calculate natural frequencies by determining the frequencies at which the reactive component of the driving impedance Z_{11} equals zero.

Note that in this approach the solution is obtained in the frequency domain. This form of solution is applicable to the steady, cyclical operation of pumps. It is not valid for transient conditions such as those occurring during rapid start-up or upset conditions. In addition, owing to assumptions inherent in the derivation of Equation (2), the technique applies to one dimensional, linear, plane-wave propagation.

The flow harmonic vector $\bar{Q}$ is obtained by discretizing the flow through the discharge or suction valve using a time-sampling technique. The sampled points are then converted from time domain to the frequency domain using standard fast Fourier transform (FFT) routines. Different harmonics in this flow spectrum are then multiplied by the corresponding impedance matrix according to Equation (A-14) to yield the pressure pulsation spectrum. This spectrum is then plotted or printed to identify significant pulsation harmonics. At the same time, pressure spectrum at the valve covers and other desired points are converted back to pressure-time arrays through the use of inverse FFT. New flow harmonics, resulting from pressure variations in the suction and discharge piping are now obtained through repeating the pump simulation and the process iterated until convergence is achieved.

When detailed valve data is not available, perfect (or ideal) valves may be assumed. This option considerably speeds up the solution and is useful during parametric studies or during the initial stages of design when final valve selection has not been done. The ideal valve assumption implies that the valves open and close instantly and perfectly. Therefore the flow through the valve is governed by the piston motion, i.e.,

$$Q = -A_p r \left[\sin\theta - \frac{r}{2l} \sin 2\theta \right] \text{ if } P > P_d$$

$$= 0 \text{ otherwise} \tag{3}$$

for a discharge valve. Flow-time relationships for an ideal valve (with fluid compressibility effects included) are compared with a real valve in Figure 4. The primary features suppressed by the ideal valve assumption are the overshoot and associated oscillations at the instant of valve opening and the small amount of backflow during closing. However, if the real valves do not function properly and flutter, the valve flow profiles will mirror the valve motion irregularities and the ideal valve assumption will then no longer be a valid approximation. For these reasons, digital or analog techniques that do not model exact valve characteristics will, in some cases, give incorrect results.

Numerical Procedure

The computer program based on the theory described above consists of two distinct parts, pump simulation and piping simulation. The interaction between the pump and
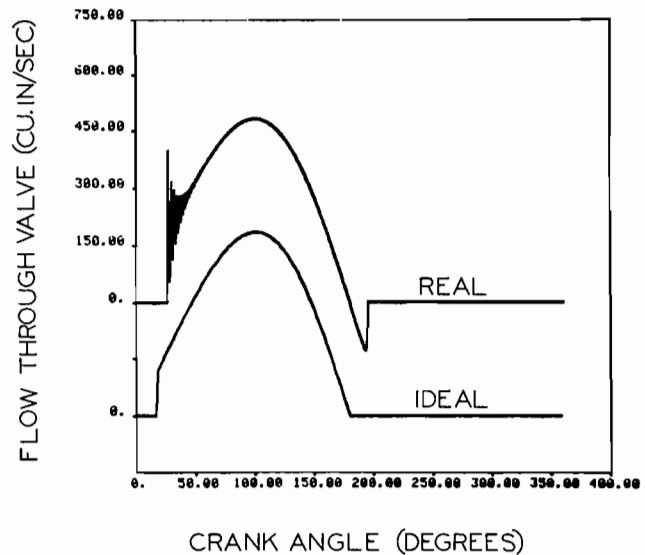

Figure 4. Comparison of Flow-time Relationships for a Real and Ideal Discharge Valve. Note that the origins are shifted along the ordinate.

the piping is achieved by an iterative procedure. The pump simulation results in the calculation of intermittent or pulsating flow through the suction and discharge valves. This flow then acts as the driving force for generating pressure pulsations in the piping. These pulsations again influence valve motion and cylinder pressures and in turn modify the flow through the valves. The various steps in this iterative process can be listed as follows:

• Calculate cylinder pressure, valve motion and flow through the valves assuming constant nominal inlet and discharge pressures.

• Calculate natural frequencies of the suction and discharge piping systems and the driving impedances of the piping at the valve covers and at other defined points in the system.

• Calculate the pressure pulsation spectrum at every desired point in the piping system. Also compute time-pressure histories at all valve covers.

• Recalculate cylinder pressure, valve motion and flow through the valves based on the new valve cover pressures.

• Recompute pressure pulsations at the valve covers and at other desired points. Compare these pulsations to those calculated in the last iterations and repeat the entire process until the pulsations and other important system parameters converge.

For the pump simulation, the Equations (A-1) through (A-7) are simultaneously integrated with proper initial conditions to calculate cylinder pressure, flow through suction and discharge valves, and valve motion. A second-order Euler integration scheme is used with roughly 25 integration steps per degree of crank rotation. It is very essential that a robust integration scheme be used with a fine enough step size to prevent numerical errors from swamping the solution and giving rise to spurious oscillations that mask the true solution.

PROGRAM VALIDATION— TEST DATA COMPARISONS

Predictions of the program have been compared to available field and laboratory test data in several cases.

Valve Motion

Valve motion data is very difficult to obtain under regular operating conditions. Fortunately, some linear variable differential transformer (LVDT) field data on the motion of suction and discharge poppet valves for a horizontal, triplex slurry pump was available for the research.

The program predicted and measured discharge and suction valve lift at 1753 psig discharge pressure and 137 cpm are compared in Figure 5. The agreement is quite good. Both measurements and computer predictions show the valves lifting fully up to the stop plates and valve closing being delayed. The amount of delay, an important parameter in valve design, is also correctly predicted.
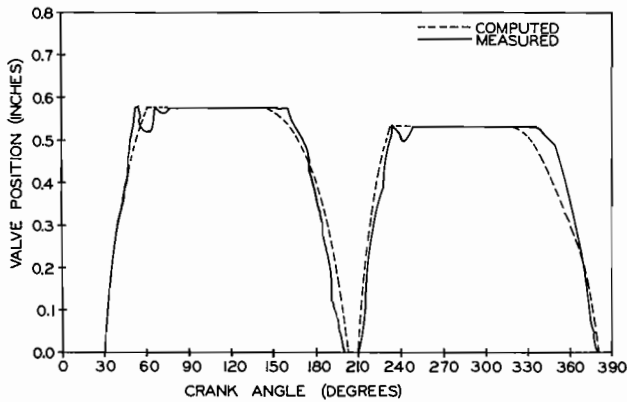

Figure 5. Comparison of Measured and Predicted Suction and Discharge Valve Lift Profiles for a Horizontal, Triplex Slurry Pump. Discharge pressure is 1753 psig and pump speed is 137 cpm.

Similar valve lift comparisons at part flow conditions of 74 cpm and 732 psi discharge pressure are shown in Figure 6. Here again, the predicted valve opening and closing angles agree well with the measured values. The lift profiles have similar shapes. Although the predictions show higher overall lift values, both the test data and the calculations indicate that the valves never lift up to the stop plates.

NPSHR

Most manufacturers quote pump NPSHR based on the Hydraulic Institute Standards [20]. In accordance with these standards, NPSHR tests can be conducted by throttling the
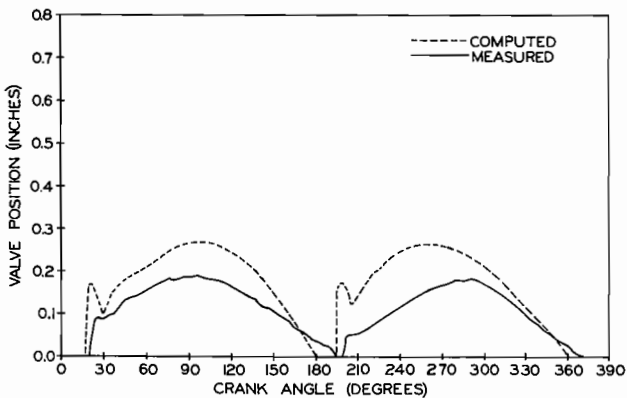

Figure 6. Comparison of Measured and Predicted Suction and Discharge Valve Lift Profiles for a Horizontal, Triplex Slurry Pump. Discharge pressure is 732 psig and pump speed is 74 cpm.

suction while holding discharge pressure and pump speed constant until either a three percent loss in capacity occurs or cavitation noise is clearly audible.

Pump capacity is plotted as a function of suction pressure over a range of operating speeds, 165 cpm to 300 cpm (Figure 7). Excellent agreement is noted between the values predicted by the program and the measurements. Particularly encouraging is the fact that the computer program correctly predicts the sharp capacity drop-off point as well as the rate of drop-off. Both the test data and measurements indicate a gradual increase in the NPSHR with increasing pump speed, as is to be expected. In addition, this program allows the user to determine NPSHR for fluids other than water (i.e., slurries, hydrocarbons, CO_2, etc).
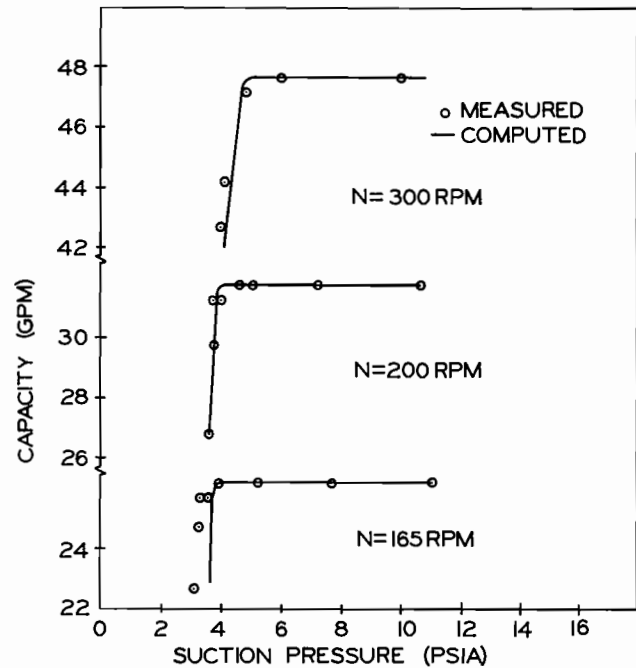

Figure 7. Comparison of Measured and Predicted NPSHR.

Piping System Natural Frequencies

As an initial check on the accuracy of the computer model, available experimental data [21] on the natural frequencies of several piping arrangements was compared to the computer predictions. The basic arrangement and pertinent dimensions are shown in Figure 8. The data was obtained in stationary air and the various end conditions can either be classified as open (large volume or atmosphere) or closed. The predicted and measured natural frequencies are listed in Table 1. The comparison is very good, with the predictions lying within 1.5 percent of the measured values.

Complete Pump Piping System Simulation

A final validation of the program was carried out by simulating a complete reciprocating pump installation

Table 1. Comparison of Predicted and Measured Piping Natural Frequencies. The measured data are taken from the literature [21].

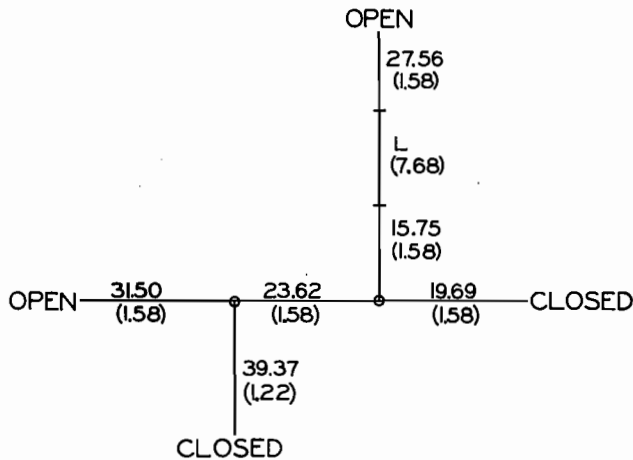| Order	Case 1, L = 3.94		Case 2, L = 7.87		Case 3, L = 8.11	
	Measured	Computed	Measured	Computed	Measured	Computed
1	38	38.2	31	30.8	26	26.3
2	68	67.0	65	63.5	63	62.2
3	106	105.8	103	101.9	101	100.6
4	145	144.7	145	144.5	145	144.4

Figure 8. Schematic Diagram Showing Piping Arrangement for Natural Frequency Calculation. Dimensions shown in inches are length and diameter (in parenthesis). Length L is variable and is defined in Table 1.

where extensive field measurements had been made. A schematic drawing of this installation is shown in Figure 9. The installation consists of roughly 20 horizontal, triplex pumps, used to pump boiler feed water for high pressure steam generation. The steam is then injected underground for secondary oil recovery.
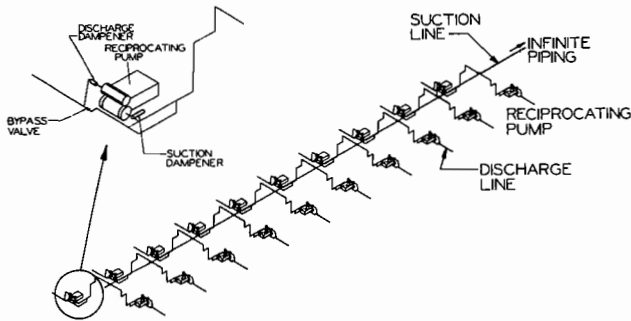

Figure 9. Schematic Diagram of a Boiler Feedwater Pumping Station.

In order to simulate complete pumping stations with multiple number of pumps, the phase angle relationship between the different pumps is required in addition to that between the cylinders of each pump. This relationship is difficult to measure and further, varies with time due to slight differences in pump speeds. Therefore, it is necessary to assume a certain phase relationship between the various pumps. Generally, all pumps are assumed to run in phase with the expectation that the additive effect will yield the worst-case scenario. This is not necessarily true for all points in the system. For detailed investigations, a few other combinations should also be tried.

The measured and predicted cylinder pressure traces, compared over one cycle of crank rotation, are shown in Figure 10. Overall agreement between the two traces is quite good with both showing the same trends. The computer model predicts the timing and the rate of rise and drop in cylinder pressure quite well. The pressure profiles during the discharge and suction strokes are also predicted remarkably well, considering the complexity of manifold piping and the rest of the piping system. The predictions closely track the phase relationship of the pressure pulsations during the

discharge stroke. The program does, however, overpredict the pressure spikes during the opening of both discharge and suction valves. This overprediction is unusual, since for most cases the program tends to underpredict these spikes. The correct prediction of high frequency spikes requires a very detailed knowledge of valve and sealing surface characteristics which are often not available. In addition, experimental investigations are being conducted to refine the model in this area.
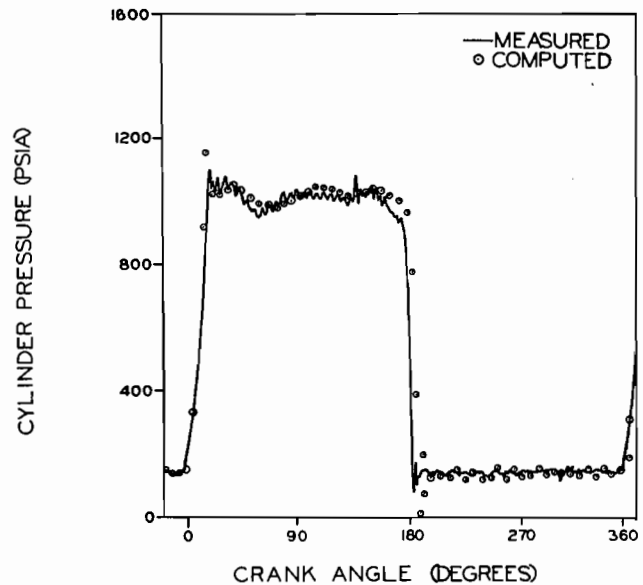

Figure 10. Comparison of Predicted and Measured Cylinder Pressure Histories.

The measured low level, high frequency pulsations during the discharge stroke are beyond the 200 Hz frequency limit set for the computer predictions. The program can predict higher frequencies (within the limits of plane-wave assumptions), but accurate calculation of these frequencies requires a much more precise knowledge of the piping dimensions and characteristics than was available in this case. Pressure pulsations at various locations in the suction and discharge piping were also predicted and compared to the measurements. An example of such a comparison at a point just downstream of the discharge flange is shown in Figure 11.
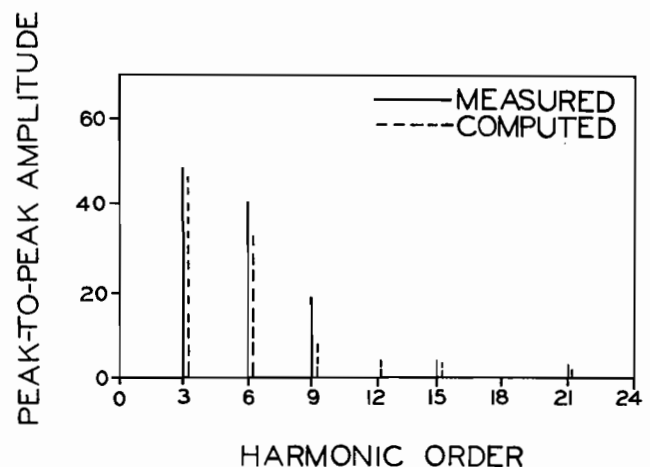

Figure 11. Comparison of Predicted and Measured Pressure Pulsations at a Point Near the Discharge Flange. The peak-to-peak pressure amplitudes are in psi.

The peak-to-peak amplitudes are high for the third and sixth harmonics, and predicted values are in close agreement with the field measurement. At other locations, although not shown here, good agreement was also obtained.

FIELD EVALUATION STUDIES

One of the main capabilities of the present program is its application in solving existing field problems and eliminating future ones. The program has been quite successful in this regard. Two case studies involving different aspects of the program are presented here to provide a flavor of the capabilities of the program.

Valve Improvement

Original valve selection for the pumps used in the installation shown in Figure 9 was done on the basis of experience before any computer program to simulate valve dynamics was available. These pumps operate satisfactorily and the noise level, although noticeable, is typical of industry practices. However, a general design review of several valve types based on the use of the program indicated that the valves used in the above mentioned pumps could benefit from improved dynamics.

The predicted valve motion is shown in Figures 12 and 13. A plot of the suction and discharge valve lift is featured in Figure 12, the corresponding valve velocities are shown in Figure 13. It is clear from these figures that both suction and discharge valves close late, with the impact velocities at the seat being relatively high. For example, the discharge valve in Figure 12 closes at 195 degrees, while compared to an ideal closing angle of 180 degrees. This delay causes some backflow into the cylinder resulting in a loss of capacity. In addition, the opening of the suction valve is equally delayed by 15 degrees. When the suction valve does open, the piston velocity is higher than it would be if the valve had opened without any delay. This higher velocity requires greater suction inflow to avoid cavitation a condition that can only be met by additional NPSHA. Thus, delay in the discharge valve closing produces higher seat impact velocities and associated noise, along with a greater suction underpressure spike. A similar effect, i.e., a higher impact velocity and larger overpressure spike, is experienced by the discharge valve because of significant delay in the suction valve closing.

As a result of these unfavorable computer predictions, the valve design and dimensions were altered and spring stiffness increased. The discharge and suction valve lift and velocity are shown, respectively, in Figures 14 and 15, for the
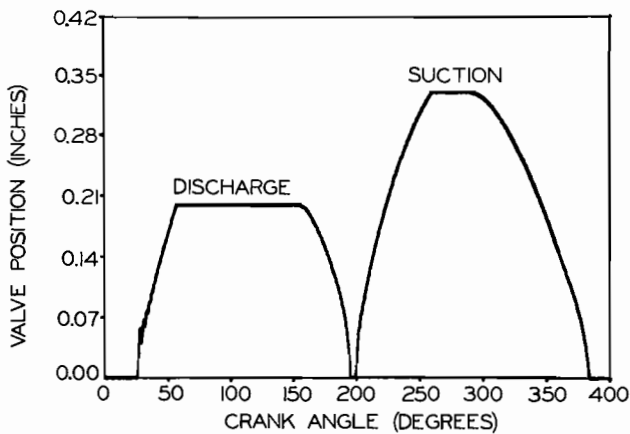

Figure 12. Suction and Discharge Valve Position as a Function of Crank Angle for Original Valve Design.
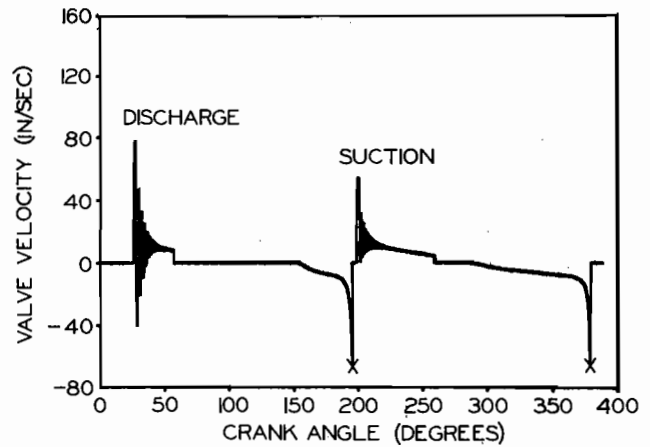

Figure 13. Suction and Discharge Valve Velocity as a Function of Crank Angle for Original Valve Design. The Xs mark the impact of the valves with their seats. The impact velocities are -71 and -65 in/sec. for the discharge and suction valves, respectively. The negative sign denotes the direction of motion is toward the seat.
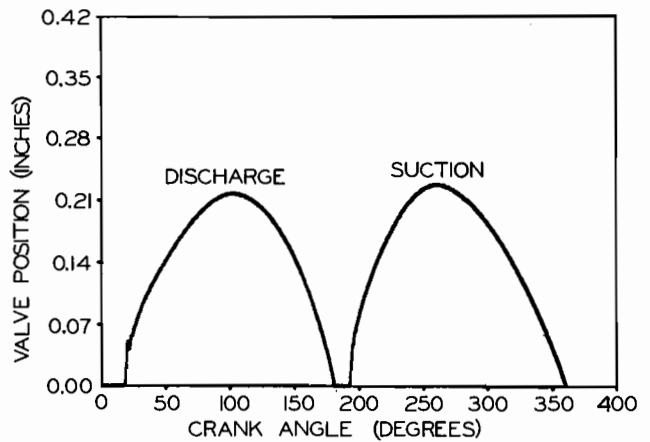

Figure 14. Suction and discharge valve position as a function of crank angle for improved valve design.
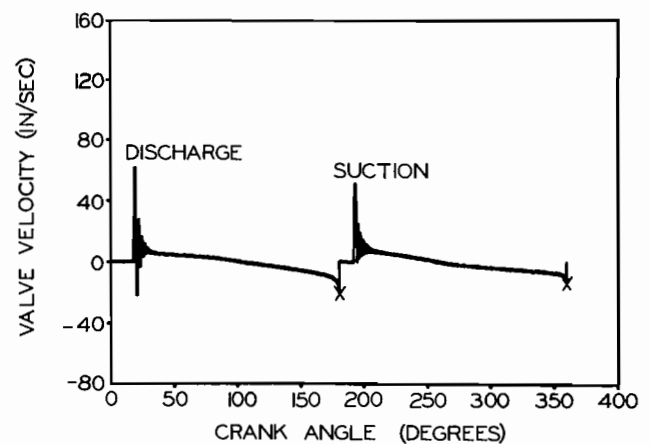

Figure 15. Suction and Discharge Valve Velocity as a Function of Crank Angle for Improved Valve Design. The Xs mark the impact of the valves with their seats. The impact velocities are -20 and -12 in/sec. for the discharge and suction valves, respectively.

new valve design. These figures indicate timely closing of both suction and discharge valves and a factor of four reduction in seat impact velocities (marked by Xs in Figures 13 and 15) over the original valves.

The predicted improvements in the new design were verified in the field. While it was not feasible to measure valve lift and velocity, the vertical accelerations on the top of the suction and discharge manifolds at the midsection were measured with the old and new valves installed in the pump. The measurements for the old and new valve designs are presented in Figures 16 and 17, respectively. It is clear from
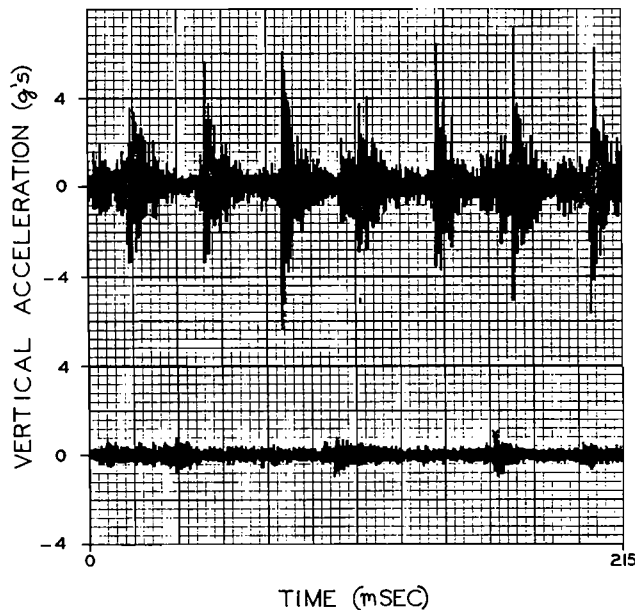

TIME (mSEC)

Figure 16. Measured Vertical Accelerations on Top of the Suction Manifold at the Midsection with Original (above) and Improved (below) Valve Designs Installed in the Pump.
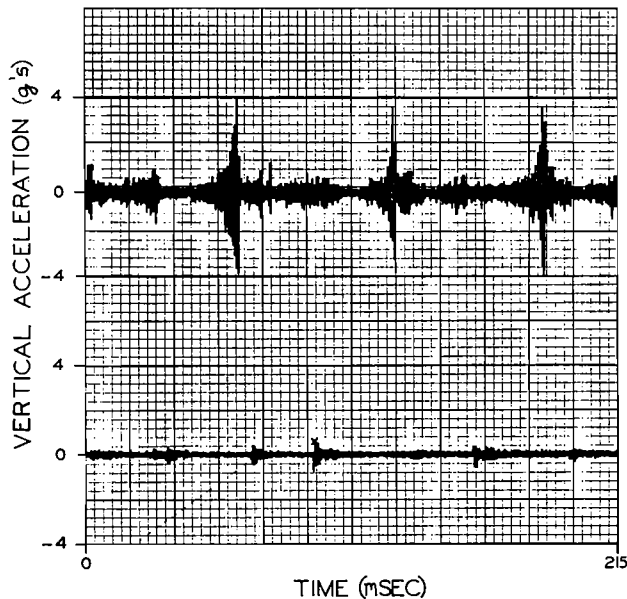

TIME (mSEC)

Figure 17. Measure Vertical Acceleration on Top of the Discharge Manifold at the Midsection with Original (above) and Improved (below) Valve Designs Installed in the Pump.

these figures that the use of the new valves significantly reduced surface accelerations and vibrations. Field observations also indicated considerable attenuation, in fact, a near total elimination, of valve noise and a reduction in suction and discharge piping pulsations.

It may be mentioned that a small delay (up to five degrees) in closing of either the suction and discharge valve is not very detrimental. In some cases, it may actually be helpful. For pumps operating over a wide range of speeds and pressures, the valve closing angle will vary slightly over the operating range. Thus, a valve that closes with, say, a five degree delay at 300 cpm may actually close perfectly at 200 cpm. On the other hand, if the valve closed perfectly at 300 cpm, the valve may start to close early at 200 cpm. This generally results in pressure build-up in the cylinder and valve bounce-back. The valve will then have an undesirable tendency to have multiple impacts, some of these impacts being with very high velocities. This can result in loud noise, valve failure and cavitation.

Piping Pulsations

Ten quintuplex pumps are used in another overseas location to pump water underground in an oil field for secondary recovery. These pumps were exhibiting both suction and discharge piping vibrations and pump component failures. Measurements at the site [22] showed that both suction and discharge piping were experiencing resonant pulsations in the 100 Hz frequency range. The computer model was used first to validate these measurements and then to evaluate the effectiveness of several proposed solutions. Plots of predicted and measured peak-to-peak pulsations at three locations in the discharge piping are shown in Figure 18. Measured pulsation spectra for pump speeds varying between 250 cpm to 300 cpm are shown on the right. The corresponding predictions are shown along side on the left. While the format of the measurement and computer plots are different, they both tell the same story.

In the computer plots, the pump speed is varied from 240 cpm to 300 cpm at 10 cpm intervals and the resulting pulsation amplitudes are connected for each harmonic. Both the measurements and predictions indicate two resonances at about 70 Hz and 90 Hz and high pulsation levels up to these resonances are excited by the fifteenth and twentieth harmonics of flow pulsations. The measurements also indicate that the pulsation level gradually decreases (note the different scales on the three plots of measured data) from the first point to the third point while the primary harmonics remain unchanged. The predictions show an identical trend and similar pulsation reductions.

Among the various solutions proposed to eliminate the severe pulsations problem, the simplest was to increas the system damping by installing an orifice of approximately half the pipe diameter at the discharge manifold. Computer predictions, as shown in Figure 19, suggest about a 3:1 reduction in the pulsation amplitude of the resonant harmonics without affecting the spectral distribution. Field measurements [22] made subsequent to orifice installation and shown in Figure 19 on the right also indicate a similar reduction. Results of suction piping simulation, although not presented here for the sake of brevity, produced equally good agreement.

DISCUSSION

The simulation program has been established as a valuable tool and its predictions validated as shown in the previous section. Judicious use of the simulation program, accom-
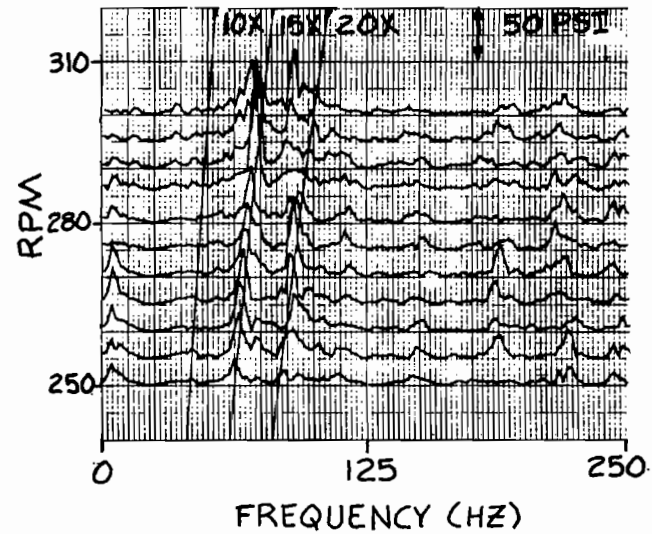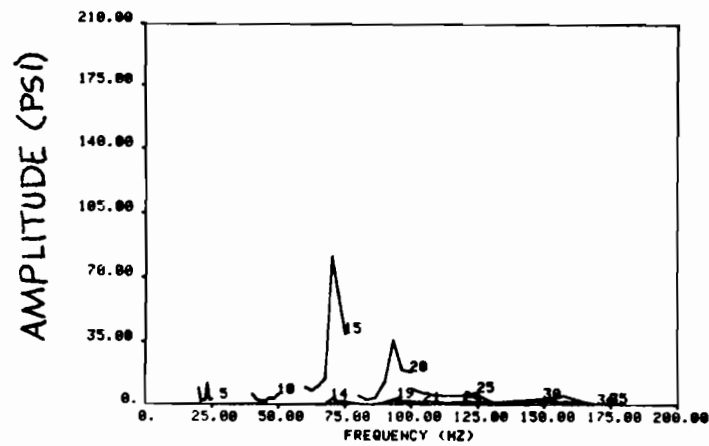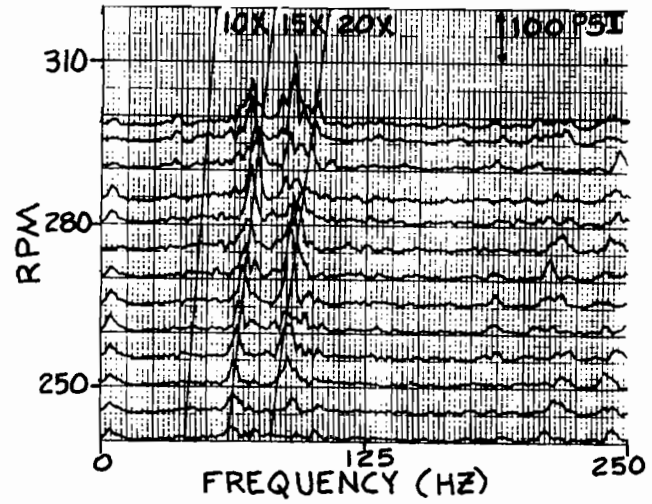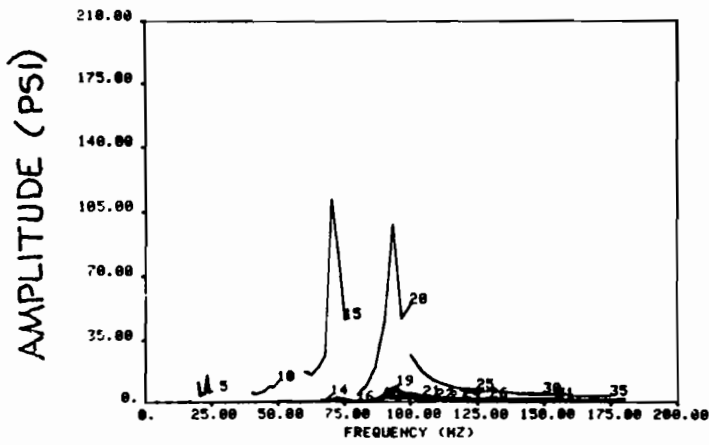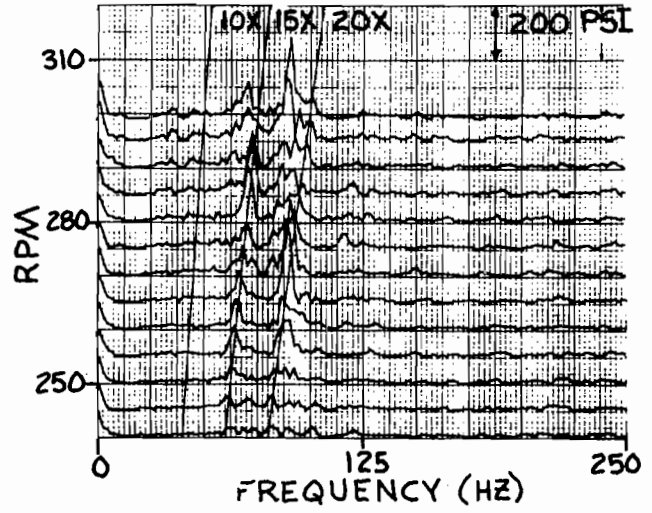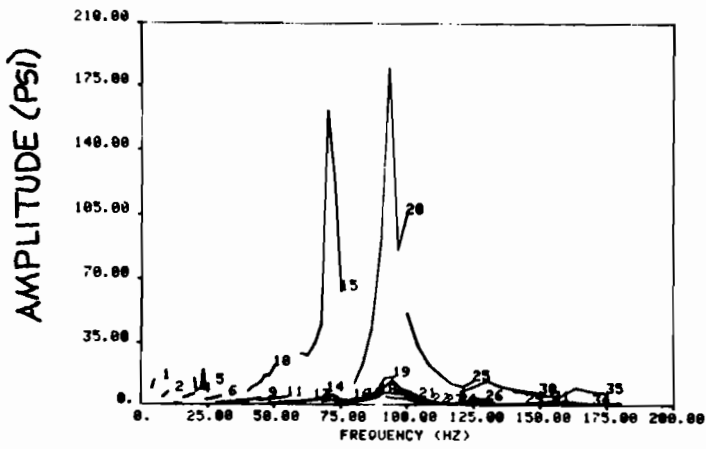
Figure 18. Computer Predictions (Left) and Field Measurements (Right) of Pressure Pulsations at Various Locations along the Original Discharge Piping. The locations (from top to bottom) correspond to the closed end of the manifold, just upstream, and just downstream of the pulsation dampener. Note that peak-to-peak amplitudes are plotted. Also, the scale varies in the plots of field data.

Figure 19. Computer Predictions (Left) and Field Measurements (Right) of Pressure Pulsations at Various Locations along the Discharge Piping with an Orifice Installed at Discharge Flange.

Locations (from top to bottom) correspond to the closed end of the manifold, just upstream of and just downstream of the pulsation dampener.

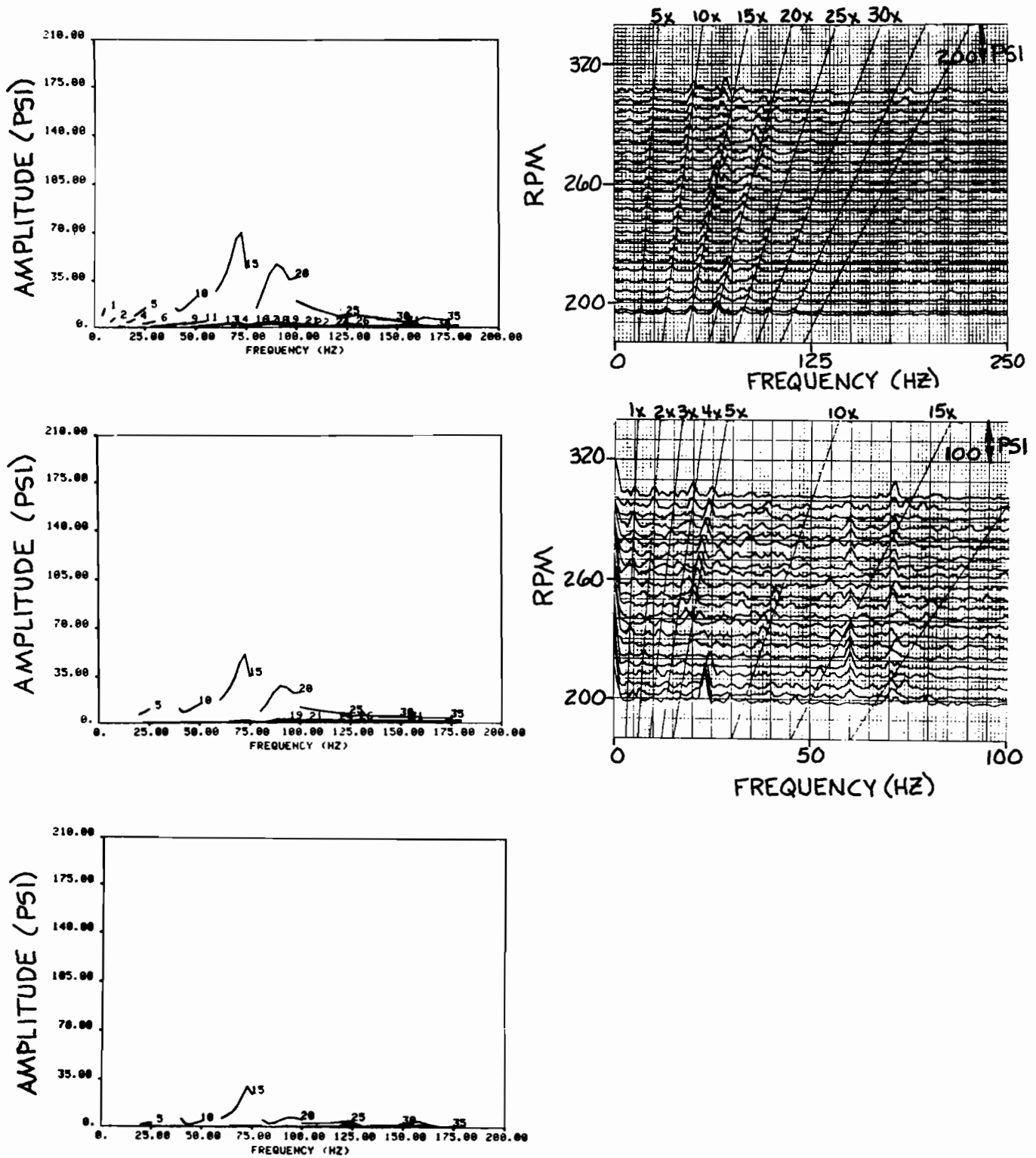panied by sound physical reasoning, can provide valuable insights leading to an enhanced understanding of pump behavior. Several such insights gained by the authors are discussed here.

Flow Excitations

As explained earlier, intermittent flow from the valves serves as an exciting force for the piping pulsations although the actual level of pulsations depends on the piping characteristics. Multiple-plunger pumps decrease the fluctuations due to overlapping of flows. The percent peak fluctuations below and above the mean flow line are shown in Table 2 for a pump with varying number of plungers and l/r (connecting rod length to crank radius) ratio of 6 (assuming incompressible fluid and ideal valves).

Table 2. Effect of the Number of Plungers on the Peak Fluctuations below and above the Mean, for a Pump with l/r = 6.

Pump type	Number of plungers	% above mean value	% below mean value	Total deviation	Crank offset
Duplex double-acting (piston)	2	24	22	46	180°
Triplex	3	6	17	23	120°
Quadruplex	4	11	22	33	90°
Quintuplex	5	2	5	7	72°
Sextuplex	6	5	9	14	60°
Septuplex	7	1	3	4	51.5°
Nonoplex	9	1	2	3	40°

The role of l/r in determining flow and pressure pulsations is generally not fully appreciated. For a very long connecting rod approaching l/r = ∞, the plunger motion would be completely sinusoidal and the valve flow would be of the form following Equation (3).

$$Q = - A_p r \, Sin\theta \text{ if } P > P_d$$

$$= 0 \text{ otherwise} \tag{4}$$

The primary flow harmonics would then be expected to correspond to multiples of the number of plungers. For example, a triplex pump will create flow harmonics of 3rd, 6th, 9th, . . ., etc., order with the third harmonic being the most prominent. However, as shown in Figure 20, the third harmonic as well as all odd multiples are all zero. Only the even multiples such as 6th, 12th, 18th harmonics have non-zero values. It can be shown mathematically that a multiple-plunger pump having large l/r ratio and pumping nearly incompressible fluid will only create even-multiple flow harmonics.

When connecting rod effects are included, i.e., l/r, odd multiples begin to emerge. Flow harmonics for a triplex pump with l/r = 5 are also shown in Figure 20. The third harmonic now is the largest of all the harmonics. Thus the crank-connecting rod mechanism is the primary source of first-multiple (often called fundamental) and other odd-multiple harmonics.

The significance of this observation lies in the fact that most gas bottles or pulsation dampeners are tuned to the fundamental frequency. In many cases, the next multiple of this frequency may be more significant. Although the frequency response of the dampeners is wide enough to cover several harmonics, the effectiveness of the dampeners can be significantly increased by tuning them to attenuate the
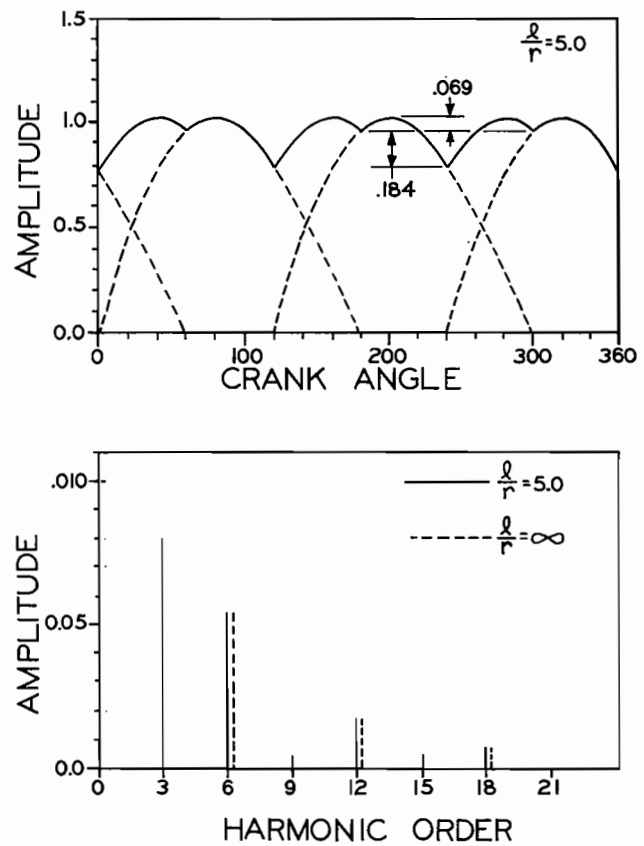

Figure 20. Pressure Amplitude Variation with Crank Angle (Top) and Corresponding Frequency Spectrum (Bottom) for a Triplex Pump Handling Incompressible Fluid.

largest harmonic. A knowledge of the significant flow harmonics is thus essential in dampener design and selection, and in avoiding resonance problems.

Cavitation

Cavitation in liquids occurs when the local static pressure falls below the liquid vapor pressure and the liquid flashes into a vaporous cavity. The extent of cavitation, particularly in time-varying flows, depends on many factors including nuclei concentration. The nuclei serve as seeds for formation of the cavitation bubbles. Abundant nuclei are usually available in the form of dissolved gas, liquid impurities, and surface imperfections. In reciprocating pumps, cavitation can occur in many regions of the pump system. The factors influencing cavitation in various regions are described forthwith.

Suction Piping

When the piping pulsations are severe or the suction pressure is low, the pulsations can locally create regions of unsteady cavitation. An example of such cavitation can be seen in the pressure trace (Figure 21) taken in the suction piping of a triplex pump. The cavitation region is identified by a flattening of the trough of the pressure trace followed by high-frequency pulsations caused by the cavitation bubbles collapsing.

The suction piping arrangement, shown in Figure 1 with some kind of pulsation dampener, is representative of current piping practices. In such an arrangement, the region first affected by cavitation is generally adjacent to the closed
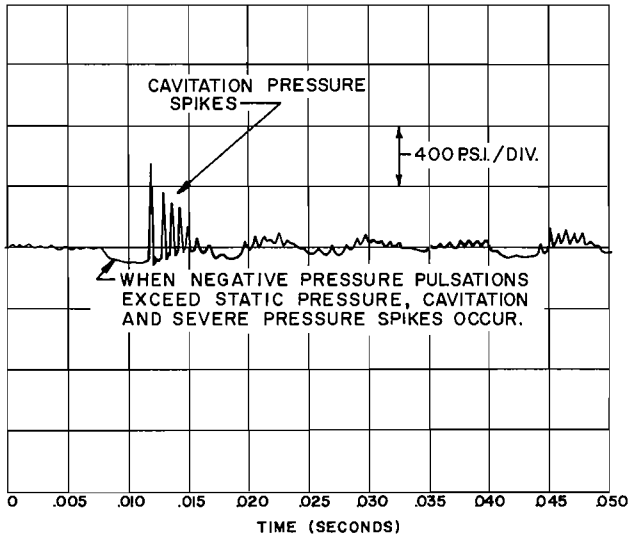
Figure 21. *Typical Pressure Signal within Suction Manifold* [23].

end of the manifold. This is due to the fact that the dampener and the closed end of manifold form a quarter wavelength resonating system with the highest pressure pulsations at the manifold end. This situation can be alleviated by moving the dampener to the closed end, in essence changing the closed end to an open end. Such a change may, however, cause the pulsations to travel through the inlet piping without attenuation. If two dampeners are used, one upstream of the pump inlet and the other at the closed end of the manifold, the maximum pulsation point may move to the center of the manifold. It is therefore very difficult to predict *apriori* what effect any piping changes will have on the acoustic pulsation without system simulation Cavitation damage within manifolds is generally not a serious problem, although high frequency pulsations caused by cavitation can result in vibrations and failure of stub attachments and drainage valves.

Suction Valve

Even when the manifold is cavitation-free, the local static pressure in the suction valve land area can easily fall below the vapor pressure. This happens in particular when the valve is about to open and the velocity through the valve is very high. In order to understand this let us temporarily ignore the inherent unsteadiness of the flow through the
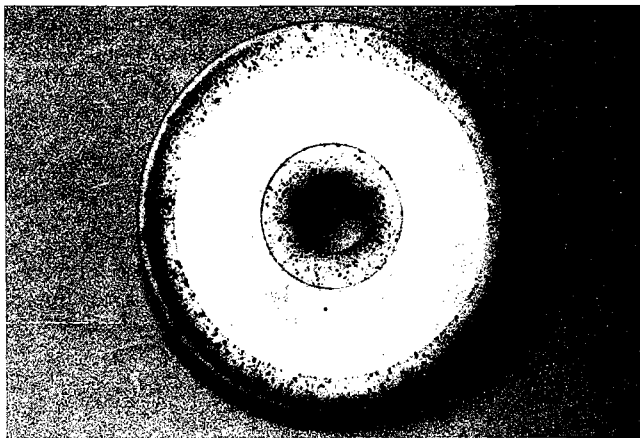

Figure 22. *An Example of Cavitation Pitting on a Suction Valve.*

valve. The pressure in the valve area is then given by the Bernoulli's equation,

$$P_{vl} = P_{su} - \frac{\rho}{2}\left(\frac{Q}{A_v}\right)^2 - P_{f1} \tag{5}$$

If $P_{vl} < P_v$, cavitation exists in the valve area as well as within the cylinder unless the valve exit passage is diffusing. As the valve area increases, the cylinder pressure begins to build up and valve flow velocity therefore decreases. The resulting increase in pressure and collapse of cavitation bubbles can then cause damage to the nearby valve face and seat area. An example of such cavitation pitting on a suction valve is shown in Figure 22.

Discharge Valve

Discharge valves are normally free of cavitation since the pressures here are much higher than the vapor pressure. However, cavitation can occur even in discharge valves during the initial lift-off phase. When the valve lifts off, the space between the land and valve seat is filled in by the surrounding fluid [24]. If the initial valve lift velocity is so large that the fluid is unable to fill the void, instantaneous pressure in this region can fall below the vapor pressure. This phenomenon generally lasts for a few microseconds, after which the pressure in the region rapidly rises to the discharge pressure. Such large, rapid pressure fluctuations can in some cases cause local cavitation-induced pitting in the mid-region of the valve land and seat area. The likelihood of cavitation is highly dependent on valve geometry, in particular the land width, surface roughness, valve dynamics, piping pulsation and many other factors. The relative importance of these factors is under investigation through mathematical modelling and evaluation of experimental data.

Cylinder

In a manner analogous to valve cavitation, if the flow rate into the cylinder is not sufficient to fill the void created by the plunger motion, the pressure inside the cylinder will fall below the vapor pressure resulting in cylinder cavitation. The additional pressure differential caused by this drop in cylinder pressure results in an increased flow rate, and the cavity collapses when the void is completely filled. This
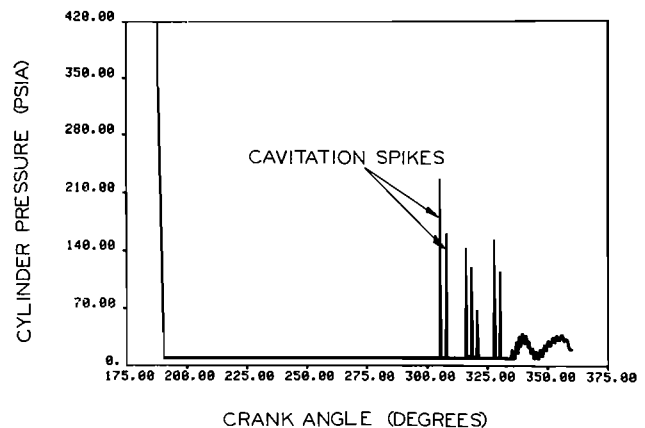

Figure 23. *Predicted Cylinder Pressure During Suction Stroke for the Pump in Figure 9 During Low Suction Pressure (22 psia) Operation. Note cavitation spikes.*

collapse results in a series of closely spaced pressure spikes, the magnitudes of which sometimes approach the discharge pressure [23]. The computer program is capable of predicting these spikes, as shown in Figure 23, although the amplitudes may not exactly match the measurements since the program does not include a bubble collapse model.

The extent of cylinder cavitation depends on the available suction head, valve dimensions and dynamics, and pump speed. Cylinder cavitation should generally be avoided because the resultant pitting can act as stress risers and cause cylinder failures. In a corrosive environment, combined corrosion and cavitation erosion can induce early structural failures.

Acceleration Head

One of the important terms in calculating piping system NPSHA is the acceleration head which, according to Hydraulic Institute Standards [20], must be added to the pump NPSHR along with frictional losses. The acceleration head is typically calculated by assuming that the entire fluid in the suction piping of the pump must be accelerated or decelerated as a block according to changes in pump flow demand. Mathematically, the acceleration head is given as

$$H_a = \frac{L}{A} \; \frac{dQ}{dt} = C_H \frac{L}{A} \; n_s Q \tag{6}$$

where C_H is a constant depending on the number of plungers. The Hydraulic Institute Standards uses the definition:

$$H_a = C_h \frac{L}{A} \; n_s Q \tag{7}$$

This relationship is essentially similar to the one given by Equation (6), except that the empirical constant C_h also accounts for the type of fluid.

Prior knowledge of the acceleration head is unnecessary if the acoustic piping simulation technique is employed, since such a simulation accounts for flow rate changes in the suction piping and for valve dynamics. Bear in mind, also, that the concept of acceleration head is valid only when the pipe length is much smaller than the wavelength of the highest frequency of concern. For longer pipes the fluid compressibility which is ignored in Equation (7), becomes significant. As an example, assuming $c = 4000$ fps, $n_s = 300$ cpm, $N = 5$, the wave length for the tenth harmonic is given as,

$$\lambda = \frac{c}{10 \; \frac{n_s}{60}} = \frac{4000}{10 \times 5} = 80 \text{ ft} \tag{8}$$

The pipe length should be typically less than $\lambda/10$ (or 8 ft.) for Equation (7) to be valid. Sometimes, the acceleration head concept is indiscriminately and incorrectly applied to pipe lengths much longer than a full wavelength. This limitation has not been clearly defined in current reciprocating pump standards. A mathematical basis for this discussion is given in Appendix B.

NPSHR

As described earlier, measured NPSHR is based on a three percent loss in pump capacity. This definition is similar to the three percent head loss criterion frequently used in the centrifugal pump industry. However, in practice, the NPSH required to achieve reliable pump operation and avoid serious cavitation is much higher than the measured NPSHR (using the three percent capacity loss yardstick), even after the acceleration head and friction losses are taken into account.

Recognize that any measurable loss in capacity caused by inadequate NPSH implies that the cylinder is cavitating through the entire suction stroke. During the discharge stroke then, the plunger idles for a while before the compression process begins, resulting in a loss in pump capacity.

To assure smooth, reliable pump operation, cavitation should be totally avoided in any part of the system. Generally, the first signs of cavitation appear inside the cylinder during the beginning of the suction stroke. Cylinder pressure measurements shown in Figure 10 for the boiler-feed triplex pump indicate a pressure spike of about 30 psi below the mean suction pressure at the instant of suction valve opening. Based on these measurements and accounting for other losses, the cavitation-free NPSHR (dubbed here as NPSHCF) would be 45 psig as compared to an NPSHR of 20 psig calculated according to Hydraulic Institute Standards (including acceleration head and other losses). This explains why pumps in the field generally operate better at suction pressures higher than the quoted NPSHR.

Another factor influencing field NPSHR measurement is the pulsations in the suction piping. In most large pump installations, some sort of pulsation dampener is generally used. This dampener if effective, reduces the first or second primary harmonics by in essence decreasing the acceleration length from the pump to the filter, thereby cutting down the pulsations being transmitted to the main piping. However, it can also create additional resonant pulsations that are generally much higher in magnitude than the first few harmonics. It is therefore essential that a complete simulation such as the one presented here be used for determining the effective NPSHA needed for cavitation free or marginal cavitation condition.

Piping Simulation

The first major step toward understanding and predicting pressure pulsations in any given piping system was taken by the reciprocating compressor industry with the introduction of the SGA Analog in the 1960s. The technique gained widespread acceptance in the compressor community and soon became the industry standard. The analog approach has also been extended to reciprocating pump piping systems. The acoustic simulation of pump suction and discharge piping to predict system response and to design a piping system free of excessive pulsations and vibrations can thus be accomplished either with digital or analog techniques. However, unlike the compressor industry where such simulation prior to installation is almost the norm, pump piping simulation has mostly been used as a corrective tool for field problems. Many of these costly problems can be avoided by proper piping design.

Pulsation Levels

One obvious question that immediately arises is what may be considered an acceptable level of pulsations. This issue can be addressed by identifying the harmful effects of pulsations on pump operation. Large pulsations create the need for additional NPSHA; otherwise, they induce cavitation in some part of the system. Another noticeable effect is piping vibrations and, sometimes, failure due to excessive dynamic stresses. The unbalanced pulsations result in a dynamic shaking force applied at those points where either the piping area or the fluid direction changes. The level of vibrations again depends on the structural response of the

piping system [25, 26] and on whether the structural resonances are being excited. The worst scenario occurs when the acoustic and structural resonant frequencies are very close. A comprehensive piping simulation should include both acoustic and structural analysis.

Certain guidelines on the level of maximum pressure pulsations, similar to those suggested by The American Petroleum Institute (API) for compressors [27], will be extremely helpful. Care should be taken, however, not to use arbitrary criteria such as one percent or two percent of line pressure. The new API guidelines proposed for compressors include limits only on individual frequency components; in fact, they suggest that the overall limits recommended earlier for some cases be completely eliminated.

A word of caution in directly applying the API guidelines for compressors to pumps. In a crude sense, the pulsation amplitude is proportional to the piping specific impedance, given as $\rho c/A$. For liquids, both the density, ρ, and the speed of sound, c, are much higher than for gases. The pipe area, A, is generally of the same order. The pulsation amplitudes would, hence, be much higher in liquids than gases for geometrically similar piping systems. Thus, while one cannot directly apply compressor guidelines to pumps, a similar approach based on pump fundamentals can certainly be developed.

In addition to this, the piping designer should follow guidelines on good piping practices [28, 29] in order to minimize the overall impact of vibrations.

Speed of Sound

It must be stressed that piping simulation does not provide a precise calculation of pulsation magnitudes. Rather, it should be viewed as an analytical tool capable of helping a designer avoid serious design mistakes. Aside from the inherent assumptions and limitations described earlier, an imprecise knowledge of fluid properties is another major contributing factor to prediction errors. To understand this effect, consider the speed of sound, c, which is a critical factor in predicting resonance frequencies. The value of c for liquids can vary widely depending on the gas content. For example, the value of c is 4500 fps for water at ambient conditions, but drops to between 2600 and 4300 fps depending on the line pressure with only 0.1 percent air content as shown in Appendix C. In order to account for these and other uncertainties, the pulsation analysis is generally performed over a 10 percent range around the nominal cpm.

System Damping

Another factor that greatly influences the magnitude of resonant pulsations is the value of system damping. While several analytical or empirical expressions for damping are available, the precise value of damping throughout the piping is not known. These limitations apply both to digital and analog simulation although the digital technique offers better control in handling them.

These limitations, however, do not detract from the vast usefulness of the technique in eliminating or solving system problems—they are mentioned here in order to maintain perspective.

Digital vs Analog Approach for Piping Simulation

As mentioned earlier, the SGA Analog has been used for several years to model compressors and pump piping systems. The analog in its present form cannot provide detailed simulation of the pump itself; therefore, this discussion is restricted to the simulation of the piping system only.

Both digital and analog techniques, if properly applied, can be very useful in piping system design and, in fact, are highly recommended. Since the terms digital and analog in the context of piping analysis sometimes create confusion among readers, the two approaches are compared here for the sake of clarity:

• Both techniques essentially solve the linearized wave equation. Digital methods use a distributed impedance approach, while the analog uses the so-called lumped impedance approach. In the latter, the piping is divided into small sections roughly one foot in length and each section is simulated by an analogous impedance element.

In the digital transfer matrix method, there is no restriction on the length of the piping element.

• The SGA analog does not account for the connecting rod length effect (l/r ratio) in its cylinder model. As explained earlier, this effect can be quite important, particularly for pumps, in the calculation of flow excitation harmonics.

• Digital techniques do not require any special hardware unlike the analog system. Any computer with sufficient memory (including some PCs) is adequate for the digital methods.

• Digital methods are generally more flexible and versatile. Model enhancements such as different kinematics or improved element modelling unlike the analog, can be easily incorporated. In addition, the digital method can be coupled directly to other computer models such as those for structural vibrations, pump simulation, etc.

• The accuracy of both methods depends on the accuracy of the input data and an understanding of their limitations. While the digital methods are inherently capable of higher accuracy, any such advantage is often overcome by inaccuracies in the input data such as the speed of sound, fluid damping and piping dimensions.

• In the digital methods, an old piping setup can be recalled from inactive storage anytime and the results can be reproduced. The analog setup, once disassembled, has to be recreated from scratch.

• Piping setup time is generally much less with the digital methods. However, the execution time for evaluating piping modifications is much less with the analog than with the digital methods. This difference depends on the speed of the digital computer being used.

CONCLUSIONS

Like most other machines, reciprocating pumps can greatly benefit from computerized design and analysis techniques.

Details of a computer program that can simulate the steady-state operation of a complete pump installation, including the piping system, have been presented here. Based on the above, the following conclusions may be reached:

• All the main characteristics of pump operation such as cylinder pressure variation, valve dynamics, cavitation, NPSHR, piping pulsations can be predicted.

• The computer predictions have been compared against laboratory and field data in several cases and shown to be in good agreement.

• The program can be useful at various stages of design from initial parametric study to the final design review. Its utility in diagnosing and solving field problems has been firmly established.

• The use of simulation techniques such as the one presented here, supplemented with knowledge gained from

experience, can lead to major advances in pump technology. It is particularly recommended that acoustic pulsation analysis, and possibly structural vibration analysis, be carried out for piping systems for all large pumps.

• Several aspects of pump operation and design that can benefit from this analytical approach have been discussed. As a result, many guidelines on common design questions such as calculation of acceleration head, NPSHR, acceptable piping pulsation levels are offered where none have existed before.

• The current NPSHR standards are generally not adequate to eliminate likelihood of serious cavitation and consequential un -smooth pump operation and cavitation damage. As an example, measurements and calculations indicate that cavitation-free NPSHR for the pump-piping system of Figure 9 is at least 45 psig. The NPSHR according to Hydraulic Institute Standard (three percent capacity loss) for the same system is computed to be less than 20 psig.

NOMENCLATURE

Nomenclature

A   Pipe cross-sectional area.
A_p Plunger cross-sectional area
A_{vl} Effective valve lift area
A_v Valve flow area at any instant.
A_{ij}, B_{ij} Four-pole matrix elements
C_{ij}, D_{ij}
c_o Velocity of sound in unbounded medium
c_m Velocity of sound in two-component mixture
c   Velocity of sound
C_D Damping force
C_1 Coulombic damping coefficient
C_2 Viscous damping coefficient
C_L Valve lift force coefficient
ds_x Differential surface element area in the x-direction
D   Plunger bore
D_p Pipe diameter
E   Young's modulus of elasticity
F   Pressure force on the valve
f   Friction coefficient
j   Imaginary number; $(-1)^{1/2}$
k   Wave number $= 2\pi/\lambda$
K   Spring force
K_o Spring preload
K_n Spring force nth polynomial coefficient
K_t Spring force transcendental term
l   Connecting rod length
L   Pipe length
M_{ij} Four-pole matrix
m   Effective valve lift element mass
m_o Valve lift element mass
m_s Spring mass
m_h Hydrodynamic added mass
n_s Pump speed in rpm
P   Cylinder pressure
P_d Discharge pressure
P_{fl} Frictional pressure drop
P_i Pressure variation harmonic at the ith point

P_L Line Pressure
P_o, P_s Pressures at zero and s distance along a streamline.
P_{su} Suction pressure
P_v Fluid vapor pressure
P_{vl} Pressure across the valve lift element surface.
Q   Volume flow rate
Q_{in} Volume flow rate into the cylinder
Q_{out} Volume flow rate out of the cylinder
r   Crank radius
S   Surface element
s   Length along the streamline
t   Time
t_p Pipe thickness
u   Fluid velocity
u_o, u_s Fluid velocities at zero and s distance along streamline.
v_{gr} Gas to liquid volume ratio
V   Cylinder volume at any instant
V_c Clearance volume
x   Valve lift at any instant
$\dot{x}$ Valve lift element velocity = dx/dt
$\ddot{x}$ Valve lift element acceleration = d^2x/dt^2
Z_{ij} Impedance matrix
ΔP Mean pressure difference across the valve.
α Damping factor
β Fluid isothermal bulk modulus
β_{is} Fluid isentropic bulk modulus
γ Damped complex wave number, $\alpha + jk$
ω Angular velocity
λ Wave length
ρ Fluid density
θ Crank angle
Σ Summation

APPENDICES

Appendix A
  Kinematics

For power pumps we can write,

$$V = V_c + A_p r \left[1 + \cos\theta + \frac{1}{r} \left\{ 1 - (1 - \frac{r^2}{l^2} \sin^2\theta)^{1/2} \right\} \right] \quad (A\text{-}1)$$

When $\frac{r}{l}$ is small, $(1 - \frac{r^2}{l^2} \sin^2\theta)^{1/2} \approx 1 - \frac{r^2}{2l^2}\sin^2\theta$

Then (A1.1) reduces to

$$V = V_c + A_p r \left[1 + \cos\theta + \frac{r}{2l} \sin^2\theta \right] \quad (A\text{-}2)$$

and

$$\frac{dV}{dt} = -A_p r \left[\sin\theta - \frac{r}{2l} \sin 2\theta \right] \quad (A\text{-}3)$$

Note that in these equations, $\theta = 0$ refers to the bottom dead center (BDC) position.

Cylinder Thermodynamics

The pressure rise in the cylinder depends on the fluid bulk modulus and the net flow in and out of the cylinder as follows:

$$\frac{dP}{dt} = \beta \left[-\frac{dV}{dt} + \Sigma(Q_{in} - Q_{out}) \right] \tag{A-4}$$

Here, ΣQ_{in} is the total flow into the cylinder which includes flow through the suction valve and leakage flows. Similarly, ΣQ_{out} is the total flow out of the cylinder. Strictly speaking, the bulk modulus, β, is a function of pressure P and temperature T, but it can be assumed to be constant, corresponding to the mean pressure and temperature with the exception of certain ultra-high pressure pumping applications.

Valve Dynamics

A damped, single degree of freedom system is used to model the valve dynamics.

$$m\ddot{x} + C_D(x,\dot{x}) + K(x) = F(x)$$

where

$$m = m_o + \frac{m_s}{2} + m_h$$

$$C_D(x,\dot{x}) = C_1\,\dot{x} + C_2\dot{x}\,|\dot{x}|$$

$$K(x) = \sum_n K_n x^n + K_t(x)$$

$$F(x) = \int_s P_{vl}\, dS_x \tag{A-5}$$

K_t represents the spring force relationship for non-coil springs which are generally represented by transcendental equations. The pressure P_{vl} around the valve lift element is determined by drawing a control volume around the element and then solving the one-dimensional Euler equation at different points along the control volume. If a quasi-steady lift coefficient $C_L(x)$ is available, then,

$$F(x) = C_L(x)\, A_{vl}(x)\, \Delta P(x) \tag{A-6}$$

Cavitation

At any point in the system, $P = P_v$ if P falls below P_v from dynamic considerations.

Flow Through Valves

Writing the unsteady Euler equation including friction loss term,

$$\frac{\partial u}{\partial t} + \frac{du^2}{2} = -\frac{1}{\rho}\frac{dP}{ds} - \frac{f}{2x}u^2 \tag{A-7}$$

Integrating (B-6) along a streamline and noting that

$$u = \frac{Q(t)}{A_v(s,t)}$$

$$\int_0^s \frac{\partial\left(\frac{Q}{A_v}\right)}{2t}\, ds + \tfrac{1}{2}(u_s^2 - u_0^2) = \frac{1}{\rho}[P_0 - P_s] - \frac{f}{2x}\int_0^s \frac{Q^2}{A_v^2}\, ds \tag{A-8}$$

This first order differential equation in dQ/dt is solved for a control volume surrounding the valve element along with equations (A-1) to (A-5) to yield cylinder pressure and Q, x, ẍ for both suction and discharge valves.

Piping Simulation

The four-pole matrix [30] for a pipe element is given by,

$$M_{12} = \begin{bmatrix} A_{12} & B_{12} \\ C_{12} & D_{12} \end{bmatrix} = \begin{bmatrix} Cosh\gamma L & \dfrac{j\omega A}{\rho c^2 \gamma}Sinh\gamma L \\ \dfrac{Pc^2\gamma}{j\omega A}Sinh\gamma L & Cosh\gamma L \end{bmatrix} \tag{A-9}$$

For a series of elements such as shown in Figure 24, the system matrix linking points 1 and 5 is given by,

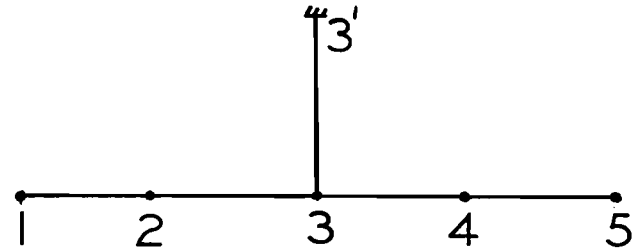$$M_{15} = M_{12}\ M_{23}\ M_{33}\ M_{34}\ M_{35} \tag{A-10}$$

Figure 24. Piping Sketch.

M_{33} is a junction matrix which is governed by the piping elements in the connecting branch. For the particular case in Figure 24 where the branch 33' ends in a closed end,

$$M_{33} = \begin{bmatrix} 1 & B_{33'}/D_{33'} \\ 0 & \end{bmatrix} \tag{A-11}$$

The valve flow Q (t) can be resolved into complex Fourier components, i.e.,

$$\bar{Q}(nw) = \sum_{n=-\infty}^{\infty} Q(t)\, e^{jn\omega t} \tag{A-12}$$

Once the system matrix M_{15} is known, it is more convenient to transfer it into an impedance matrix by the following relationship,

$$Z_{11} = \frac{D_{15}}{B_{15}};\ Z_{15} = Z_{55} = \frac{1}{B_{15}};\ Z_{55} = \frac{A_{15}}{B_{15}} \tag{A-13}$$

Then, the pressure and flow harmonics at points 1 and 5 are related as follows:

$$\begin{bmatrix} \bar{P}_1(n\omega) \\ \bar{P}_5(n\omega) \end{bmatrix} = \begin{bmatrix} Z_{11}(n\omega) & Z_{15}(n\omega) \\ Z_{51}(n\omega) & Z_{55}(n\omega) \end{bmatrix} \begin{bmatrix} \bar{Q}_1(n\omega) \\ \bar{Q}_5(n\omega) \end{bmatrix} \tag{A-14}$$

The pressure time history at points 1 and 5 can then be obtained by inverse Fourier transform of P_1 and P_5

Appendix B

Acceleration Head

For a suction pipe of length L, with one end attached to a large supply source (open end boundary conditions) and the

other end to a pump valve, the pressure pulsations at the valve from the transfer matrix theory are given by,

$$\tilde{P}_1(\omega) = Z_{11}\,\tilde{Q}_1(\omega) \tag{B-1}$$

where the subscript 1 refers to the point at the valve. The value of Z_{11} for undamped acoustic pulsations in an open-end pipe [29] is given by,

$$Z_{11} = \frac{j\rho c}{A}\,\tan kL \tag{B-2}$$

where

$$k = \frac{\omega}{c} = \frac{2\pi}{\lambda}$$

is the wave number and λ is the wave length. If $L \ll \lambda$, $kL \ll 1$, $\tan kL \approx kL$, then, (B-2) becomes,

$$Z_{11} = \frac{j\rho c}{A}\,kL = \frac{j\rho c}{A}\,\frac{\omega}{c}\,L = \frac{j\rho\omega L}{A} \tag{B-3}$$

$$\tilde{P}_1(\omega) = \frac{\rho L}{A}\,j\omega\,\tilde{Q}_1(\omega) \tag{B-4}$$

$$P_1(t) - P_o = \frac{\rho L}{A}\,\frac{dQ_1}{dt} \tag{B-5}$$

This is the same relationship as given in Equation (6) indicating that the commonly used method to calculate acceleration head and the transfer matrix method are compatible as long as $kL \ll 1$ or $L \ll \lambda/2\pi$ or ω/c.

Notice that when $L = \lambda/4$, $kL = \pi/2$, the value of Z_{11} becomes infinity. The corresponding frequency $f = c/\lambda$ is then the natural frequency of the system. The actual pulsation level does not reach an infinite value because of the system damping. When damping is included, (B-2) becomes,

$$Z_{11} = \frac{\rho c^2 \gamma}{j\omega A}\,\text{Tanh}\gamma L, \quad \gamma = \alpha + jk \tag{B-6}$$

where α is a damping factor. The actual level of pulsations at the resonant frequency depends on the value of flow harmonic at that frequency and the damping factor, α.

Note that, the commonly used technique of (B-5) cannot account for resonances at all, because it ignores the fluid compressibility.

Appendix C

Speed of Sound

The speed of sound in an unbounded liquid can be calculated from (C-1).

$$c_o = \left(\frac{\beta_{is}}{\rho}\right)^{1/2} \tag{C-1}$$

Both β_{is} and ρ are, in general, weak functions of pressure and temperature. Such dependance can be ignored for most problems where the pressure and temperature variations

from the mean values is not substantial. Values of speed of sound for water and other liquids at different pressure and temperatures can be found in [31, 32]. When the fluid is bounded, the compliance of the bounded medium also affects the value of c. For fluid in a pipe, it can be shown that,

$$c = c_o\left(1 + \frac{D_p\,\beta_{is}}{t_p E}\right)^{-1/2} \tag{C-2}$$

If the pipe is very stiff, i.e., $E\,t_p \gg D_p\beta_{is}$, the value of c is equal to c_o. The value of c in water for Schedule 40 steel pipe for various diameters is given in Table 2 ($c_o = 4900$ fps, $E = 30 \times 10^6$ psi, $\beta_{is} = 300{,}000$ psi).

Notice that as the pipe diameter increases, pipe compliance also increases and the speed of sound gradually goes down.

The value of c changes drastically if the liquid contains even small traces of gaseous or vapor phase. Following [32], it can be shown that the speed of sound c_m in a liquid-gas mixture with small amounts of gas can be derived from the following relationship:

$$\frac{c_m}{c_o} = \frac{1 + v_{gr}}{\left(1 + \frac{\beta_{is}\,v_{gr}}{P_L}\right)^{1/2}} \tag{C-3}$$

where $v_{gr} = v_g/v_l$ is the ratio of gas volume to liquid volume. Table 3 outlines the drastic reduction in the speed of sound in water with the amount of entrained air ($\beta_{is} = 300{,}000$ psi)

Experimental data of Karplus [34] for the speed of sound in water containing air bubbles verifies the rapid decline in sound speed with an increase in air content. At $v_{gr} = 0.10$, the data shows that $c = 100$ fps and at $v_{gr} = 0.3$, $c = 60$ fps. These are much lower than even the speed of sound in pure air. Beyond $v_{gr} = 0.90$, the value of c rises rapidly again towards the pure air value.

Table 3. *Variation of the Speed of Sound with Pipe Diameter (Schedule 40 Pipe) for Water.*

Nominal Pipe Size (In)	Inside Dia. (In)	Thickness (In)	c (Ft/Sec)
2	2.067	0.154	4601
3	3.068	0.216	4585
4	4.026	0.237	4530
5	5.047	0.258	4481
6	6.065	0.280	4442
8	7.981	0.322	4386
10	10.02	0.365	4340
12	11.938	0.406	4307

Table 4. *Effect of Undissolved Air Content on the Speed of Sound in Water.*

Entrained Air (% by Volume)	Speed of Sound (fps)	
	$P_L = 100$ psig	$P_L = 1000$ psig
0	4900	4900
0.1	2580	4308
0.5	1312	3128
1.0	950	2488

Appendix D

The system simulation computer program described in the text is written in a highly structured, user-friendly and flexible format. Some commonly used options of the program are:.

- Pump performance with or without piping.
- Valve motion and impact studies.
- Pump NPSHR evaluation.
- Pump cavitation evaluation.
- Piping simulation using ideal valves.
- Complete pump simulation including suction and discharge piping.
- Complete pumping station evaluation.

Input to the program mainly consists of fluid properties, and cylinder, valve, and piping dimensions. Program output is in the form of multiple print and plot data files. Several print files, each with a specific form of output, are automatically generated. The salient print output variables are listed below:

Performance

- Indicated and total horsepower.
- Capacity and volumetric efficiency.
- Capacity loss due to backflow.

Valve Dynamics

- HP loss due to valve restriction.
- Opening and final closing angles.
- Stop and seat impact velocities (i.e., velocities just before impact).
- Maximum valve velocity.
- Number of impacts on the stop and seat plates.
- Valve natural frequency.

Piping Dynamics

- Piping natural frequencies up to a specified limit.
- Ten highest valve flow harmonics and phase angles.
- Ten highest pressure harmonics and phase angles at all specified pulsation points.

All significant output data is also available in the form of plots. The complete simulation of a triplex pump, including valve effects and system piping requires about three minutes of CPU time per iteration on a PRIME 750 computer. Generally, three iterations are adequate for complete convergence. For piping simulation, using ideal valves, the CPU time reduces to 10 seconds.

REFERENCES

1. Miller, J. E., "Liquid Dynamics of Reciprocating Pumps-2 Pulsation-Control Devices and Techniques," Oil & Gas Journal (May 2, 1983).

2. Nimitz, W., and Damewood, G. "Compressor Installation Design Utlizing an Electro-Acoustic System Analog," ASME Paper 61-WA-290 (1961).

3. Von Nimitz, W. W., "Reliability and Performance Assurance in the Design of Reciprocating Compressor and Pump Installations," Proceedings of the Purdue Compressor Technology Conference, Purdue University (1974).

4. Wachel, J. C., Szenasi F. R., and Denison, S. C., "Analysis of Vibration and Failure Problems in Reciprocating

Triplex Pumps for Oil Pipelines," ASME 85-Pet-10 (1985).

5. Singh, P. J., "A Digital Reciprocating Compressor Simulation Program Including Suction and Discharge Piping," International Compressor Engineering Conference, Purdue University (1984).

6. Kinsler, L. E., and Frey, A. R., *Fundamentals of Acoustics*, 3rd Ed, New York: John Wiley & Sons (1982).

7. Brunner, W., "Simulations of a Reciprocating Compressor on an Electronic Analog Computer," ASME Paper No.58-A-146 (1958).

8. Singh, R., and Soedel, W., "Mathematical Modeling of Multicylinder Compressor Discharge System Interactions," Journal of Sound and Vibration, *63* (1979).

9. Grover, S. S., "Analysis of Pressure Pulsations in Reciprocating Compressor Piping Systems," Journal of Engineering for Industry (May 1966).

10. Baumeister, K. J., "Numerical Techniques in Linear Duct Acoustics—A Status Report," Journal of Engineering for Industry, *103* (1981).

11. Baumeister, K. J., "Time Dependent Difference Theory for Noise Propagation in a Two-Dimensional Duct," AIAA Journal, *18*, (12) (1980).

12. Craggs, A., "A Finite Element Method for Damped Acoustic Systems: An Application to Evaluate the Performance of Reactive Mufflers," Journal of Sound and Vibration, *48*, (3) (1976).

13. Steyer, G. C., Puckett, S. J, and Roeder, J., "Compressor Vibration and Performance Problems Using a New Digital Computer-based Approach," Presented at 63rd Annual GPA Convention, New Orleans, Louisiana (March 1984).

14. Benson, R. S., and Ucer, A. S., "Pressure Pulsations in Pipe Systems With Multiple Reciprocating Air Compressors and Receivers," Journal of Mechanical Engineering Science, *15*, (1) (1973).

15. Lampton, M., "Transmission Matrices in Electroacoustics," Acoustica, *39* (1978).

16. To, C. W. S., and Doige, A. G., "A Transient Testing Technique for the Determination of Matrix Parameters of Acoustic System, Parts I and II," Journal of Sound and Vibration, *62*, (2) (1979).

17. Chung, J. Y., and Blaser, D. A., "Transfer Function Method of Measuring In-duct Acoustic Properties, I and II," Journal of the Acoustical Society of America, *68* (1980).

Prasad, M. G., and Crocker, M. J., "Insertion Loss Studies on Models of Automotive Exhaust Systems," Journal of Acoustical Society of America, *70*, (5) (1981)

19. Singh, P. J., "Simulation of Compressor Piping Systems and Comparison With Test Data," Presented at Nova/Husky Research Corporation Seminar, Calgary, Alberta, Canada (1986).

20. Hydraulic Institute Standards, 14th ed., Hydraulic Institute, Cleveland, Ohio, pp. 235-237 (1983).

21. Sakai, T. and Mitsuhashi, K., "Study on Pulsations of Reciprocating Compressor Piping Systems, 2nd Report," Bulletin of the Japanese Society of Mechanical Engineers, *16*, (91) (1973).

22. Smith, D. R., Farnell, W. R., and Gerlach, C. R., Engi-

neering Dynamics Inc., Technical Report 85-307-1 (1985).

23. Parry, W., "System Problem Experience in Multiple Reciprocating Pump Installations," *Proceedings of the 3rd International Pump Symposium*, Turbomachinery Laboratories, Department of Mechanical Engineering, Texas A & M University, College Station, Texas (1986).

24. Boswirth, L., "Theoretical and Experimental Study on Fluid Flow in Valve Channels, Proceedings of the Purdue Compressor Technology Conference, Purdue University (1982).

25. Hatfield, F. J., Wiggert, D. C., and Otwell, R. S., "Fluid Structure Interaction in Piping by Component Synthesis," Journal of Fluids Engineering, *104* (September 1982).

26. Von Nimitz, W. W., "Pulsation and Vibration Control Requirements in the Design of Reciprocating Compressor and Pump Installations," Proceedings of the Purdue Compressor Technology Conference, Purdue University (1982).

27. API Standard 618, Reciprocating Compressors for General Refinery Service, 3rd Edition, Final Draft (1983).

28. Controlling the Effects of Pulsations and Fluid Transients, Report No. 160 (revised) SGA-PCRC Seminar, Southwest Research Institute (November 1981).

29. Wachel, J. C., "Consideration of Mechanical System Dynamics in Plant Design," ASME Paper No. 67-DGP-5 (1967).

30. Soedel, W., "Gas Pulsations in Compressor and Engine Manifolds," Purdue University (1978).

31. Wilson, J., "Speed of Sound in Distilled Water as a Function of Pressure and Temperature," Journal of Acoustical Society of America, *31* (1959).

32. Weast, R.C., *CRC Handbook of Chemistry and Physics*, Cleveland, Ohio: CRC Press, Incorporated (1978).

33. Gouse, S. W., and Brown, G. A., "A Survey of The Velocity of Sound in Two-phase Mixtures," ASME paper No. 64-WA/FE-35 (1964).

34. Karplus, H. B., "The Velocity of Sound in a Liquid Containing Gas Bubbles," COO-248, Armour Research Foundation, Illinois Institute of Technology, Chicago, IL (1958).

ACKNOWLEDGMENT